CLINICAL STUDY

Tumor Targeting and Three-Dimensional Voxel-Based Dosimetry to Predict Tumor Response, Toxicity, and Survival after Yttrium-90 Resin Microsphere Radioembolization in Hepatocellular Carcinoma

Carole Allimant, MD, Marilyne Kafrouni, MSc, Julien Delicque, MD, Diana Ilonca, MD, Christophe Cassinotto, MD, PhD, Eric Assenat, MD, PhD, Jose Ursic-Bedoya, MD, MSc, Georges-Philippe Pageaux, MD, PhD, Denis Mariano-Goulart, MD, PhD, Serge Aho, MD, PhD, and Boris Guiu, MD, PhD

ABSTRACT

Purpose: To identify predictive factors of tumor response, progression-free survival (PFS), overall survival (OS), and toxicity using three-dimensional (3D) voxel-based dosimetry in patients with intermediate and advanced stage hepatocellular carcinoma (HCC) treated by yttrium-90 (^{90}Y) resin microspheres radioembolization (RE).

Materials and Methods: From February 2012 to December 2015, 45 ^{90}Y resin microspheres RE procedures were performed for HCC (Barcelona Clinic Liver Cancer stage B/C; n = 15/30). Area under the dose-volume histograms (AUDVHs) were calculated from 3D voxel-based dosimetry to measure ^{90}Y dose deposition. Factors associated with tumor control (ie, complete/partial response or stable disease on Modified Response Evaluation Criteria in Solid Tumors) at 6 months were investigated. PFS and OS analyses were performed (Kaplan-Meier). Toxicity was assessed by occurrence of radioembolization-induced liver disease (REILD).

Results: Tumor control rate was 40.5% (17/42). Complete tumor targeting (odds ratio = 36.97; 95% confidence interval, 1.83–747; $P < .001$) and $AUDVH_{tumor}$ (odds ratio = 1.027; 95% confidence interval, 1.002–1.071; $P = .033$) independently predicted tumor control. $AUDVH_{tumor} \geq 61$ Gy predicted tumor control with 76.5% sensitivity and 75% specificity. PFS and OS in patients with incomplete tumor targeting were significantly shorter than in patients with complete tumor targeting (median PFS, 2.7 months [range, 0.8–4.6 months] vs 7.9 months [range, 2.1–39.5 months], $P < .001$; median OS, 4.5 months [range, 1.4–23 months] vs 19.2 months [range, 2.1–46.9 months], $P < .001$). Patients with incomplete tumor targeting and $AUDVH_{tumor} < 61$ Gy, incomplete tumor targeting and $AUDVH_{tumor} > 61$ Gy, complete tumor targeting and $AUDVH_{tumor} < 61$ Gy, and $AUDVH_{tumor} > 61$ Gy had median PFS of 2.7, 1.8, 6.3, and 12.1 months ($P < .001$). REILD (n = 4; 9.5%) was associated with higher dose delivered to normal liver ($P = .04$).

Conclusions: Complete tumor targeting and ^{90}Y dose to tumor are independent factors associated with tumor control and clinical outcomes.

ABBREVIATIONS

AUDVH = area under the dose-volume histogram, BSA = body surface area, DVH = dose-volume histogram, EBRT = external-beam radiation therapy, HCC = hepatocellular carcinoma, OS = overall survival, PFS = progression-free survival, RE = radioembolization, REILD = radioembolization-induced liver disease, 3D = three-dimensional, TPS = treatment planning system, V = volume, ^{90}Y = yttrium-90

From the Departments of Radiology (C.A., J.D., C.C., B.G.), Digestive Oncology (E.A.), and Hepatology (J.U.-B., G.-P.P.), Saint-Eloi University Hospital, 80 avenue Augustin Fliche, Montpellier 34295, France; Department of Nuclear Medicine (M.K., D.I., D.M.-G.), Guy de Chauliac University Hospital, Montpellier, France; Department of Statistics and Epidemiology (S.A.), University Hospital of Dijon, Dijon, France; Montpellier Cancer Research Institute (B.G.), INSERM U1194, Montpellier, France; and PhyMedExp (D.M.-G.), INSERM U1046, CNRS UMR9214, University of Montpellier, Montpellier, France. Received January 20, 2018; final revision received July 4, 2018; accepted July 5, 2018. **Address correspondence to** B.G.; E-mail: B-guiu@chu-montpellier.fr

M.K. received research grants from DOSIsoft SA (Cachan, France) for this study. None of the other authors have identified a conflict of interest.

Appendix A and Figures E1–E4 can be found by accessing the online version of this article on *www.jvir.org* and clicking on the Supplemental Material tab.

J Vasc Interv Radiol 2018; ■:1–9

https://doi.org/10.1016/j.jvir.2018.07.006

In daily practice, tumor response and clinical outcomes following radioembolization (RE) of hepatocellular carcinoma (HCC) can vary considerably, with excellent results in certain patients and no benefit from treatment in others (1,2). No survival benefit has been demonstrated so far in any phase III trial (3,4). Thus, there is an urgent need to identify predictive factors of efficacy to improve patient selection. Although there are some differences between RE and external-beam radiation therapy (EBRT), experience from the latter could be used to improve RE. Evaluation of dosimetry is central to EBRT and could be an attractive approach to understanding the differences in outcome and response following RE.

Two methods are recommended with RE using resin microspheres to calculate the activity to be injected (5): body surface area (BSA) method and partition model method. The former is semiempiric and considers only tumor and liver volumes (extrapolated from BSA), whereas the latter is based on medical internal radiation dose principles (6) and differentiates 3 discrete vascular compartments—lungs, tumor, and nontumoral liver parenchyma—and takes into account the avidity of each for albumin macroaggregates. However, the partition model method assumes that radiation is homogeneously distributed in each compartment, which actually is not the case. More recently, treatment planning systems (TPSs) have been applied to RE procedures. This approach, which has been used for many years in EBRT, allows three-dimensional (3D) dosimetry at the voxel level. A TPS can provide dose-volume histograms (DVHs) that show and measure the heterogeneity in the distribution of yttrium-90 (^{90}Y) microspheres in the different compartments. This type of dosimetric analysis could be helpful in the field of RE. The aim of this study was to evaluate 3D voxel-based dosimetry using TPS to identify the predictive factors of tumor control, survival, and toxicity in patients with HCC treated by ^{90}Y resin microspheres.

MATERIALS AND METHODS

Patient and Tumor Characteristics

The institutional review board approved this study. Written informed consent was obtained from all patients for treatment and research. From February 2012 to December 2015, all RE procedures using ^{90}Y resin microspheres for unresectable HCC performed in a single institution were analyzed. During this period, 38 patients underwent 45 RE procedures. Two thirds of the procedures (n = 31 of 45) were part of a randomized phase III trial comparing RE and sorafenib (3). Authorization for this ancillary study was obtained from the protocol promoter. Criteria for inclusion were Barcelona Clinic Liver Cancer stage C or Barcelona Clinic Liver Cancer stage B refractory to chemoembolization (ie, no objective response of the treated nodules after 2 sessions of chemoembolization), with preserved liver function (Child-Pugh status $\leq$ B7), Eastern Cooperative Oncology Group stage 0–1, and the absence of significant extrahepatic disease [lung nodules $<$ 1 cm and lymph nodes $<$ 2 cm were allowed as in the SARAH trial protocol (3)]. Patient and tumor characteristics are presented in **Table 1**.

Work-up Procedure

All procedures were performed by interventional radiologists with $>$ 10 years of experience in interventional radiology. The BSA method was used to calculate the required dose in all but 1 patient, who had an optimized dose calculation based on the partition model. More details are available in **Appendix A** (available online on the article's Supplemental Material page at *www.jvir.org*) (5,7–11).

Treatment

In 84% (38 of 45) of cases, the same interventional radiologist performed both the work-up before treatment and the treatment procedure. Procedures were lobar (n = 36), segmental (n = 7), or whole-liver (n = 2) treatments. When the tumor had invaded both lobes, treatment was performed with segmental split injections during the same procedure (n = 5) or sequential lobar treatments (n = 4).

3D Dosimetry on Positron Emission Tomography/Computed Tomography after ^{90}Y Injection

A positron emission tomography (PET)/computed tomography (CT) scan was performed within 24 hours after ^{90}Y injection (acquisitions of 2 bed positions, 40 minutes on a Biograph PET/CT [Siemens Healthcare, Erlangen, Germany]) of all procedures. Dosimetry at the voxel level was retrospectively calculated in all patients using a TPS (PLANET Dose; DOSIsoft, Cachan, France). A radiologist with 5 years of experience in liver imaging who was not involved in the treatment procedures manually segmented the liver and tumors of all patients on the baseline CT scan using the AW Workstation (GE Healthcare, Waukesha, Wisconsin) for the purpose of the study. Baseline magnetic resonance imaging (available in 40 of 45 treatments) and imaging follow-up were also used to delineate tumors.

^{90}Y PET/CT images were co-recorded with baseline CT scan images in the TPS by a medical physicist and analyzed together with a nuclear medicine physician specializing (4 years of experience) in RE. Necrosis as a result of previous ablation or transarterial chemoembolization treatments was subtracted from the tumor and liver volume (V) so that only viable tumor and functional nontumoral parenchyma were considered. Treated liver volume ($V_{\text{irradiated liver}}$) was extracted from the TPS considering the lowest relevant isodose curve.

The nontumoral volume within the treated liver volume ($V_{\text{nontumoral irradiated}}$) was obtained by subtracting tumor volume (V_{tumor}) from $V_{\text{irradiated liver}}$ for toxicity assessment. DVHs of each anatomically defined volume (V_{tumor} and $V_{\text{nontumoral irradiated}}$) were obtained. Area under the dose-volume histogram ($AUDVH_{\text{tumor}}$ and $AUDVH_{\text{nontumoral irradiated}}$), expressed in

Table 1. Patient and Tumor Characteristics

Clinical Variable	Value
Treatments, n	45
Patients, n	38
Age, y, median ± SD	64 ± 11
Sex, n (%)	
Male	42 (0.93)
Female	3 (0.07)
Underlying liver disease, n (%)	
Alcohol	20 (0.44)
Hepatitis C	12 (0.27)
Hepatitis B	2 (0.04)
Hemochromatosis	2 (0.04)
Nonalcoholic steatohepatitis	6 (0.13)
Noncirrhotic	3 (0.07)
Child-Pugh score, n (%)	
A5	27 (0.60)
A6	12 (0.27)
B7	6 (0.13)
Performance status/ECOG, n (%)	
0	35 (0.78)
1	10 (0.22)
BCLC classification, n (%)	
B	15 (0.33)
C	30 (0.67)
Tumor distribution, n (%)	
Unifocal/multifocal	10/35 (0.22/0.78)
Unilateral/bilateral	19/26 (0.42/0.58)
Tumor phenotype, n (%)	
Infiltrative	26 (0.58)
Focal/encapsulated	19 (0.42)
Tumor size, cm, mean (range)	5 (2.8–11.44)
Prior therapy, n (%)	
Chemoembolization (transarterial chemoembolization)	23 (0.51)
Resection/ablation	18 (0.40)
Sorafenib	2 (0.04)
Combined treatments	17 (0.38)
None	15 (0.33)
AFP, n (%)	
< 200 ng/mL	36 (0.80)
≥ 200 ng/mL	9 (0.20)
Portal vein invasion	
Yes/no	20/25 (0.44/0.56)
Main	8 (0.18)
Right branch	5 (0.11)
Left branch	5 (0.11)
Segmental	2 (0.04)

AFP = α-fetoprotein; BCLC = Barcelona Clinic Liver Cancer; ECOG = Eastern Cooperative Oncology Group.

Gy, was calculated to measure the exposure of each tissue to ^{90}Y radiation (Fig 1a–d). More details are available in Appendix A (available online on the article's Supplemental Material page at *www.jvir.org*) (5,7–11).

Endpoints

Complete Tumor Targeting. Complete tumor targeting was defined as when 100% of V_{tumor} was included in the ^{90}Y-perfused volume ($V_{irradiated\ liver}$) (Fig 1a–d). Four cases of bilateral HCC were treated by 2 separate injections over an interval of 2–4 months. Targeting was considered to be complete when 100% of V_{tumor} was treated after both injections.

Tumor Control. All patients underwent a clinical examination and follow-up imaging with multiphasic CT scan 1, 3, and 6 months after treatment. Tumor control (complete/partial response or stable disease) was assessed on Modified Response Evaluation Criteria in Solid Tumors (12) after 6 months owing to the initially inflammatory changes and the well-known delayed response following RE (13). In patients who died within 6 months after treatment (n = 13), the most recent available examination was considered (median 2.5 months; range, 1–3 months). The evaluation was performed independently and blindly to clinical and follow-up data by two radiologists (5 and 6 years of experience in liver imaging). Any discordant case was reanalyzed until a consensus was reached. In the 4 cases with bilateral HCC, the response at 6 months to the first treatment was evaluated in the first treated part of the liver only. The response to the second treatment at 6 months was evaluated in the whole liver.

Progression-Free Survival. Progression-free survival (PFS) was defined as the time of the treatment procedure (the first one if repeated treatments) to disease progression or death.

Overall Survival. Overall survival (OS) was defined as the time of the treatment procedure (the first one if repeated treatments) to death (by any cause).

Toxicity. Clinical and biologic data were retrospectively collected at baseline and at 1-month intervals following treatment for up to 3 months. Liver toxicity was assessed clinically (ascites, esophageal varices, hemorrhage, hepatic encephalopathy) and biologically: albumin, total bilirubin, creatinine, international normalized ratio, and Child-Pugh and Model for End-stage Liver Disease scores were calculated. Liver toxicity was documented according to Common Terminology Criteria for Adverse Events v4.0 criteria (14). Suspected toxicity was considered to be present in the absence of progressive hepatic disease. Radioembolization-induced liver disease (REILD) was defined according to the definition by Sangro et al (15) (Table 2).

Statistical Analysis

First, mean $AUDVH_{tumor}$ in patients with tumor control was compared with mean $AUDVH_{tumor}$ in patients with progressive disease using the Mann-Whitney test. Then,

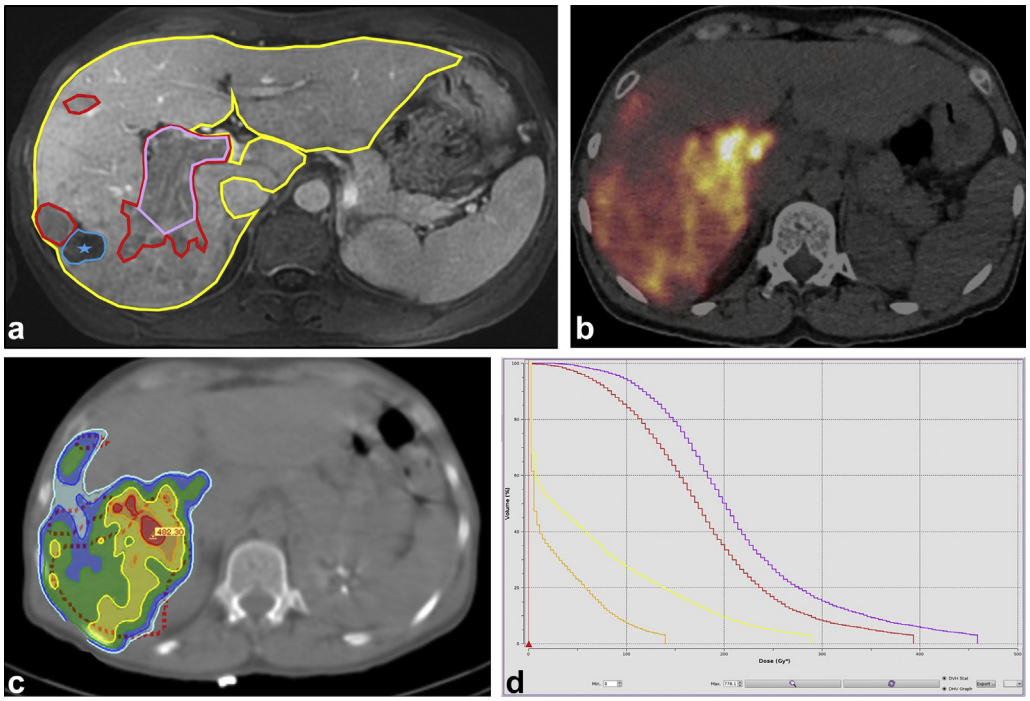

Figure 1. Example of TPS post-processing to obtain 3D voxel-based dosimetry and corresponding DVHs. **(a)** Baseline CT scan with manual segmentation of tumor (red), portal vein invasion (purple), and liver (yellow). We subtracted necrosis owing to previous ablation (blue). **(b)** ^{90}Y PET/CT imaging. **(c)** Screenshot of 3D voxel-based dosimetry with isodose curves on TPS (complete tumor targeting). **(d)** DVHs for tumor (red), portal vein invasion (purple), nontumoral irradiated liver (orange), and whole liver (yellow).

univariate and multivariate logistic regression were performed to compute corresponding odds ratios with 95% confidence intervals. Log-linearity was checked using fractional polynomials. Second, the dose-response relationship was determined using a nonlinear regression model (9). Several theoretical models were evaluated, including log-logistic with 4 or 5 parameters, Gompertz with 3 or 4 parameters, and exponential with 2 or 3 parameters. A model using fractional polynomials was also evaluated. The models were compared using residual variance Akaike information criterion. The most parsimonious model was adopted for these criteria. Receiver operating characteristic analysis was then performed to identify the optimal cutoff (defined by the Youden index) of AUDVH to predict tumor control. Finally, survival curves were estimated using the Kaplan-Meier method and compared using the log-rank test. All analyses were performed using Stata 14 (StataCorp LP, College Station, Texas) and R software (R Foundation for Statistical Computing, Vienna, Austria). $P < .05$ was considered to be significant. More details regarding statistical methodology are presented **Appendix A** (available online on the article's Supplemental Material page at *www.jvir.org*).

RESULTS

For dosimetric and survival analysis, 42 procedures in 37 patients were considered (**Fig 2**). More details are available in **Appendix A** (5,7–11) and **Figures E2–E4** (available online on the article's Supplemental Material page at *www.jvir.org*).

Table 2. REILD Criteria as Defined by Sangro et al (15)

4–8 weeks after treatment
Jaundice and ascites
Total bilirubin > 3 mg/dL or > 50 μmol/L
Elevation of GGT or ALP
No significant modification on AST/ALT
No tumor progression
No biliary obstruction

ALT = alanine aminotransferase; ALP = alkaline phosphatase; AST = aspartate aminotransferase; GGT = γ-glutamyltransferase; REILD = radioembolization-induced liver disease.

Complete Tumor Targeting, Tumor Control, and Tumor Dose

Complete targeting was obtained in 60% of cases (n = 25 of 42). All patients with incomplete targeting had disease progression within 6 months. Incomplete targeting (n = 17 of 42) was explained by the following: (*a*) very limited contralateral disease (ie, representing < 5% of total tumor volume) that was not treated to limit radiation exposure in the nontumoral liver (n = 16 of 17); (*b*) too selective treatment (n = 1 of 17) that did not fully cover all HCC nodules. An example of incomplete targeting is illustrated in **Figure E1a–c** (available online on the article's Supplemental Material page at *www.jvir.org*).

The 6-month tumor control rate was 40.5% (n = 17 of 42), including 1 patient with complete response, 12 patients with partial response, and 4 patients with stable disease

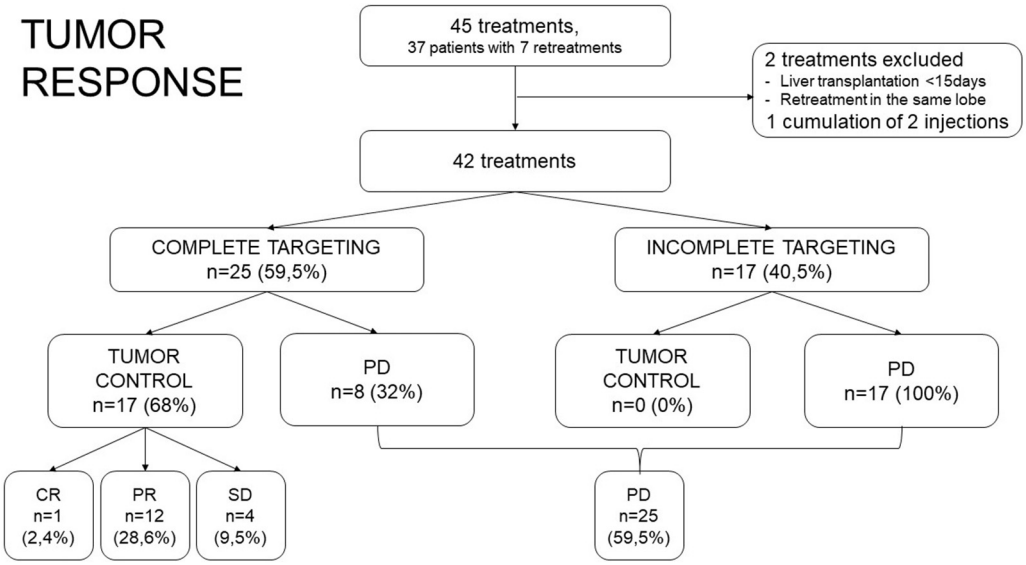

Figure 2. Flow chart showing complete targeting and tumor response. CR = complete response; PD = progressive disease; PR = partial response; SD = stable disease.

(Fig 2). Patient and tumor characteristics did not differ between the tumor control and the progressive disease group (Table 3).

The median administered activity calculated using the standard BSA method was 1.16 GBq (range, 0.29–2.11 GBq). The activity injected for the patient according to the partition model was 2.59 GBq. Mean dose deposition in all tumors in patients, represented by $AUDVH_{tumor}$, was 64 Gy ± 39. If only completely targeted patients were considered, the mean $AUDVH_{tumor}$ was significantly higher in the tumor control than in the progressive disease group (92 Gy ± 44 vs 43 Gy ± 18, $P = .0052$). Individual and model DVHs according to tumor control are presented in Figure 3a, b. Model DVHs significantly differed in the progressive disease vs tumor control groups ($P = .01$).

Complete tumor targeting and $AUDVH_{tumor}$ were significantly associated with tumor control on univariate logistic regression analysis, in contrast to age, sex, Child-Pugh status, Barcelona Clinic Liver Cancer stage, α-fetoprotein, multifocality, Eastern Cooperative Oncology Group status, prior therapy, and portal vein invasion. On multivariate analysis, both complete tumor targeting and $AUDVH_{tumor}$ independently predicted tumor control (Table 4). The area under the receiver operating characteristic curve of $AUDVH_{tumor}$ for predicting tumor control was 0.853 (95% confidence interval, 0.696–1). The optimal AUDVH cutoff was 61 Gy resulting in 76.47% sensitivity and 75% specificity for predicting tumor control (Fig E2 [available online on the article's Supplemental Material page at *www.jvir.org*]).

Survival Analysis

Median OS and PFS for the whole population was 10.2 months and 3.1 months, respectively. PFS and OS in patients with incomplete tumor targeting was significantly shorter (median PFS 2.7 months [range, 0.8–4.6 months] and median OS 4.5 months [range, 1.4–23 months]) than in patients with complete tumor targeting (median PFS 7.9 months [range, 2.1–39.5 months] and median OS 19.2 months [range, 2.1–46.9 months]) ($P < .001$ and $P < .001$ respectively) (Fig 4a–c). PFS and OS were significantly longer in patients with tumor control (median PFS 12.1 months vs 3 months, $P < .001$; median OS 24 months vs 6.5 months, $P = .002$) than in patients without tumor control. Patients with incomplete tumor targeting and $AUDVH_{tumor} < 61$ Gy, incomplete tumor targeting and $AUDVH_{tumor} > 61$ Gy, complete tumor targeting and $AUDVH_{tumor} < 61$ Gy, and complete tumor targeting and $AUDVH_{tumor} > 61$ Gy had median PFS of 2.7 months, 1.8 months, 6.3 months, and 12.1 months ($P < .001$) (Fig 4a–c).

Toxicity

Symptoms including fatigue, nausea, and abdominal pain were not examined in this study. No radiation pneumonitis was observed. One case of arterial spasm with gastroduodenal artery reflux occurred leading to duodenal radiation exposure observed on ^{90}Y PET/CT (calculated duodenal dose = 25.3 Gy). The patient presented 1 month after treatment with acute epigastric pain and anorexia owing to a large duodenal bulb ulcer (Forrest III) that was treated medically by high-dose proton pump inhibitors and eradication of *Helicobacter pylori*. Full symptomatic and endoscopic recovery occurred 8 months later.

Liver decompensation owing to RE (considering grade 3 or higher toxicity in tumor-controlled patients) occurred in 5 patients (11.9% of all treatments) (Fig E4 [available online on the article's Supplemental Material page at *www.jvir.org*]). Four patients responded to REILD criteria (9.5% of all treatments), and 1 patient had biliary obstruction. All patients died within 4 months after treatment.

Table 3. Patient Characteristics according to Tumor Control (CR+PR+SD) and Progressive Disease

Characteristic	CR+PR+SD	PD	*P* Value
Number (%)	17 (40)	25 (60)	
Age, y, median ± SD	67.5 ± 8	61.2 ± 12	.09
Sex, n (%)			.64
Male	16 (94)	23 (92)	
Female	1 (6)	2 (8)	
Underlying liver disease, n (%)			
Alcohol	7 (41)	10 (40)	1
Hepatitis C	4 (24)	8 (32)	1
Hepatitis B	2 (12)	0 (0)	1
Hemochromatosis	2 (12)	0 (0)	1
Nonalcoholic steatohepatitis	1 (6)	5 (20)	.37
Noncirrhotic	1 (6)	2 (8)	1
Child-Pugh score, n (%)			
A5	13 (76)	12 (48)	.11
A6	4 (24)	8 (32)	.73
B7	0 (0)	5 (20)	.07
Performance status/ ECOG, n (%)			1
0	13 (76)	18 (72)	
1	4 (24)	7 (28)	
BCLC classification, n (%)			.33
B	8 (47)	7 (28)	
C	9 (53)	18 (72)	
Tumor distribution, n (%)			
Unifocal/multifocal	6 (35)/11 (65)	3 (12)/22 (88)	.12
Unilateral/bilateral	10 (59)/7 (41)	7 (28)/18 (72)	.06
Prior therapy, n (%)			
Chemoembolization (transarterial chemoembolization)	12 (71)	10 (40)	.07
Resection/ablation	9 (53)	6 (24)	.1
Sorafenib	0 (0)	2 (8)	.51
Combined treatments	7 (41)	6 (24)	.31
None	2 (12)	13 (52)	.01
Portal vein invasion, n (%)			
Yes/no	7 (41)/10 (59)	11 (44)/14 (56)	1
Main	2 (12)	6 (24)	
Right branch	2 (12)	2 (8)	
Left branch	1 (6)	3 (12)	
Segmental	2 (12)	0 (0)	

BCLC = Barcelona Clinic Liver Cancer; CR = complete response; ECOG = Eastern Cooperative Oncology Group; PD = progressive disease; PR = partial response; SD = stable disease.

Patients with REILD criteria received a mean dose of 78.9 Gy in the nontumoral irradiated liver ($AUDVH_{nontumoral\ irradiated}$) (**Table 5**), which was significantly greater than the mean dose in patients without REILD criteria (53.8 Gy; $P = .04$). There was no significant difference in the mean volume of nontumoral irradiated liver or in the percentage of irradiated liver parenchyma. Patients with REILD criteria had higher baseline bilirubin levels than patients without (mean 1.73 mg/dL and 1.12 mg/dL, respectively; $P = .04$).

DISCUSSION

This study confirms the importance of tumor targeting when performing RE. Tumor targeting may be incomplete for many reasons, such as difficult catheterization, presence of an extrahepatic feeder, safety considerations to spare the nontumoral liver, and poor patient selection. Cone-beam CT or CT angiography can be of great help as they are during transarterial chemoembolization by providing precise arterial mapping and identifying extrahepatic feeders (16). Although tumor response was recently suggested as a valid endpoint (17), RE has been considered to be only palliative treatment so far. For palliative treatments, tumor control (with a preserved quality of life) remains the main goal (18). For these reasons, tumor control was chosen as the main endpoint.

The second independent criterion predicting tumor control was the dose delivered to the tumor. Many retrospective studies, which have been clearly summarized in a review by Cremonesi et al (19), showed a good correlation between the mean absorbed dose in the tumor and the response to RE. The dose threshold to predict tumor control was 61 Gy for AUDVH with a specificity and sensitivity of 75%. This is difficult to compare with other studies because of different dose calculation methods or different endpoints. For example, in a similar population (n = 73 patients), Strigari et al (20) used ^{90}Y bremsstrahlung imaging to calculate mean tumor dose and showed that a 110-Gy threshold led to objective response in 74% of patients. All patients in the present study underwent imaging after treatment with PET/CT, which provides higher spatial resolution and more accurate quantitative data than ^{90}Y bremsstrahlung single photon emission computed tomography (SPECT) imaging (21). Imaging and quantification after ^{90}Y treatment is an exceptional situation in radio-oncology, as, in contrast to EBRT, it gives an overview of the dose deposition in tissue and allows a direct evaluation of dose effect.

Many authors more recently have focused on evaluation of DVHs. In contrast to the partition model, which incorrectly assumes that there is a uniform dose distribution, DVH analysis takes into account the heterogeneous deposition of ^{90}Y microspheres (22). Kao et al (23) introduced the notion of D70 (the minimum absorbed dose delivered to 70% of the tumor), which is already used in EBRT, and V100 (the percentage of the tumor volume receiving $\geq$ 100 Gy). Based on a very small cohort (n = 7 patients with HCC), they found that a complete response was generally obtained when D70 was > 100 Gy. In a small cohort of 26 patients, Fowler et al (24) presented a DVH graph that was similar to ours in both primary and secondary liver tumors with ^{90}Y PET/magnetic resonance imaging 3D dosimetry. This study analyzed only the mean dose and D70 and found

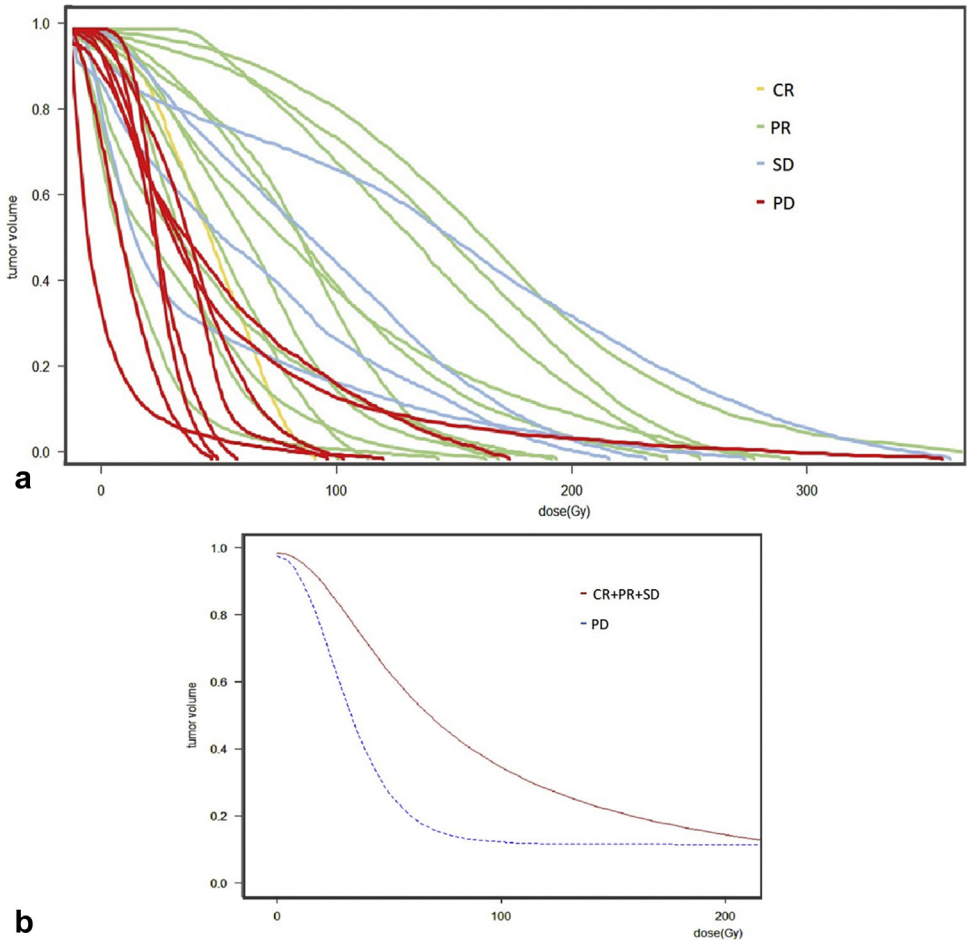

Figure 3. **(a)** DVHs of all 25 patients with complete targeting. **(b)** Model DVHs of tumor control vs progressive group ($P = .01$). CR = complete response; PD = progressive disease; PR = partial response; SD = stable disease.

Table 4. Univariate and Multivariate Analysis of Tumor Control

	Univariate		*P* Value	Multivariate		*P* Value
	OR	95% CI		OR	95% CI	
Age	1.069	0.993–1.152	.078			
Complete targeting	60.790	3.01–1227.16	< .001*	36.97	1.83–747.6	< .001*
$AUDVH_{tumor}$	1.043	1.017–1.083	.008*	1.027	1.002–1.071	.0325*
Sex	1.391	0.116–16.677	.794			
Child (B vs A)	0.25	0.158–2.426	.232			
AFP (≥ 200 ng/mL vs < 200 ng/mL)	0.71	0.32–2.182	.118			
Multifocal/unifocal	0.25	0.051–1.217	.086			
Portal vein invasion	0.694	0.195–2.472	.573			
Prior treatment	3.67	0.823–16.332	.088			
BCLC (C vs B)	0.72	0.23–2.387	.489			
ECOG (1 vs 0)	0.58	0.168–1.87	.399			

AFP = α-fetoprotein; AUDVH = area under the dose-volume histogram; BCLC = Barcelona Clinic Liver Cancer; CI = confidence interval; ECOG = Eastern Cooperative Oncology Group; OR = odds ratio.
*Statistically significant.

that responders significantly differed from nonresponders except for patients with HCC given the small population size. AUDVH mathematically provides a better reflection of the actual dose received by the tumor than the commonly used mean dose, which does not take into account the heterogeneity of dose deposition. Of 42 cases, 3 were identified with poor agreement between AUDVH and the mean dose (overestimation by 200% using the mean dose).

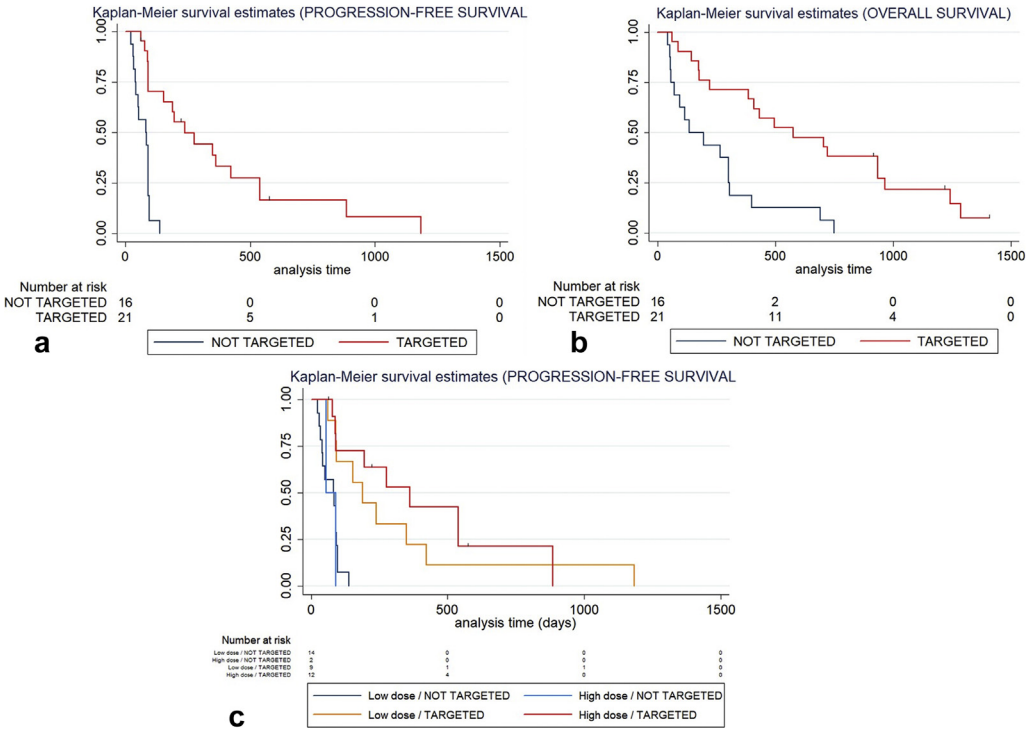

Figure 4. Kaplan-Meier estimates. **(a)** PFS in patients with complete vs incomplete tumor targeting ($P < .001$). **(b)** OS in patients with complete vs incomplete tumor targeting ($P = .001$). **(c)** PFS in patients depending on tumor targeting and a 61-Gy cutoff for $AUDVH_{tumor}$ ($P < .001$).

Because of the importance of complete targeting and tumor dose, special attention must be paid to toxicity. REILD is the critical level of toxicity in RE that results in severe and sometimes fatal consequences (15). Because most HCCs occur in patients with cirrhosis, it is difficult to determine whether liver decompensation is due to natural worsening of underlying liver function, disease progression, or treatment. Any adverse events that occurred within 3 months after treatment in the absence of tumor progression were considered to be treatment-related adverse events (25). Liver decompensation was defined as grade 3 or greater toxicity in Common Terminology Criteria for Adverse Events, resulting in a rate of toxicity of 11.9% (n = 5 of 42), which is close to the 8.5% reported by Garin et al (25) (n = 6 of 71) using the same definition. REILD occurred in 9.5% of patients (n = 4 of 42) in the present study, which is higher than the reported incidence rate of 0%–4% in large RE cohorts with mixed tumor types (15). However, if only HCC occurring in cirrhotic patients is considered, REILD was reported at a similar rate as in our study in the study by Gil-Alzugaray et al (26) (9.3% in 260 patients with comparable characteristics).

Normally, REILD should be related to both the percentage of treated liver and the dose delivered to the nontumoral liver. Although no difference was observed in nontumoral treated volumes, there was a higher dose deposition in the nontumoral liver in patients with REILD compared with others ($P = .04$). The dose in the nontumoral liver was > 58 Gy in all patients with REILD. In EBRT (27), 55 Gy is the limit for one third of total liver irradiation (which is comparable to RE in the left lobe) and 45 Gy for two thirds of the total liver (approximately equal to the right lobe) with a 50% probability of significant liver toxicity. In a previous study evaluating RE with resin microspheres for HCC, a dose > 52 Gy was associated with a 50% probability of complications based on the linear-quadratic radiobiologic model (20).

Table 5. REILD versus No REILD Dose and Volume in Nontumoral Irradiated Liver

Disease Controlled	No REILD	REILD	*P* Value
Number	14	4	
AUDVH nontumoral irradiated, Gy, mean	53.84	78.91	.04
Volume nontumoral irradiated, cm^3, mean	484	441	NS
Volume non tumoral irradiated, %, mean	32	30	NS

AUDVH = area under the dose-volume histogram; NS = not significant; REILD = radioembolization-induced liver disease.

This study has several limitations, including its retrospective design and its low number of patients. Also, evaluation of Modified Response Evaluation Criteria in Solid Tumors may be difficult because of inflammatory response, ill-defined boundaries in infiltrative disease, and previously treated HCC with necrotic areas. This is the reason tumor control, which is easier to define, was chosen as the main endpoint. Heterogeneous dose calculation methodology was used, as all patients except 1 were treated based on BSA

method. Additionally, the BSA method may result in underdosing tumors, as previously demonstrated (28,29). Finally, this study focused only on the delivered dose based on ^{90}Y PET/CT. Although this makes it possible to evaluate actual delivered doses, dose prediction based on macroaggregated albumin SPECT results is crucial. However, the ability of macroaggregated albumin SPECT to actually predict the delivered dose is still a subject of debate in the literature (30).

In conclusion, complete tumor targeting and 3D voxel-based tumor dose represented by $AUDVH_{tumor}$ are independent factors associated with tumor control and clinical outcomes. Data collection regarding both complete targeting and tumor dose should be encouraged in ^{90}Y RE studies to validate these potential predictive factors.

REFERENCES

1. Sangro B, Carpanese L, Cianni R, et al. Survival after yttrium-90 resin microsphere radioembolization of hepatocellular carcinoma across Barcelona Clinic Liver Cancer stages: a European evaluation. Hepatology 2011; 54:868–878.
2. Salem R, Gordon AC, Mouli S, et al. Y90 radioembolization significantly prolongs time to progression compared with chemoembolization in patients with hepatocellular carcinoma. Gastroenterology 2016; 151: 1155–1163.e2.
3. Vilgrain V, Pereira H, Assenat E, et al. Efficacy and safety of selective internal radiotherapy with yttrium-90 resin microspheres compared with sorafenib in locally advanced and inoperable hepatocellular carcinoma (SARAH): an open-label randomised controlled phase 3 trial. Lancet Oncol 2017; 18:1624–1636.
4. Chow PKH, Gandhi M, Tan SB, et al. SIRveNIB: selective internal radiation therapy versus sorafenib in Asia-Pacific patients with hepatocellular carcinoma. J Clin Oncol 2018; 36:1913–1921.
5. Lau WY, Kennedy AS, Kim YH, et al. Patient selection and activity planning guide for selective internal radiotherapy with yttrium-90 resin microspheres. Int J Radiat Oncol Biol Phys 2012; 82:401–407.
6. Ho S, Lau WY, Leung TWT, et al. Partition model for estimating radiation doses from yttrium-90 microspheres in treating hepatic tumours. Eur J Nucl Med 1996; 23:947–952.
7. Bolch WE, Bouchet LG, Robertson JS, et al. MIRD pamphlet No. 17: the dosimetry of nonuniform activity distributions—radionuclide S values at the voxel level. Medical Internal Radiation Dose Committee. J Nucl Med 1999; 40:11S–36S.
8. D'Arienzo M, Chiaramida P, Chiacchiararelli L, et al. 90Y PET-based dosimetry after selective internal radiotherapy treatments. Nucl Med Commun 2012; 33:633–640.
9. Ritz C, Baty F, Streibig JC, Gerhard D. Dose-response analysis using R. PLoS One 2015; 10:e0146021.
10. Bland JM, Altman DG. Statistical methods for assessing agreement between two methods of clinical measurement. Lancet 1986; 1:307–310.
11. Lin LI. A concordance correlation coefficient to evaluate reproducibility. Biometrics 1989; 45:255–268.
12. European Association for the Study of the Liver; European Organisation for Research and Treatment of Cancer. EASL–EORTC Clinical Practice Guidelines: management of hepatocellular carcinoma. J Hepatol 2012; 56:908–943.
13. Atassi B, Bangash AK, Bahrani A, et al. Multimodality imaging following 90Y radioembolization: a comprehensive review and pictorial essay. Radiographics 2008; 28:81–99.
14. National Cancer Institute Common Terminology Criteria for Adverse Events. CTCAE_4.03_2010-06-14.xls. Available at: https://evs.nci.nih.gov/ftp1/CTCAE/About.html. Accessed June 14, 2010.
15. Sangro B, Gil-Alzugaray B, Rodriguez J, et al. Liver disease induced by radioembolization of liver tumors. Cancer 2008; 112:1538–1546.
16. Bapst B, Lagadec M, Breguet R, Vilgrain V, Ronot M. Cone beam computed tomography (CBCT) in the field of interventional oncology of the liver. Cardiovasc Intervent Radiol 2016; 39:8–20.
17. Riaz A, Gabr A, Abouchaleh N, et al. Radioembolization for hepatocellular carcinoma: statistical confirmation of improved survival in responders by landmark analyses. Hepatology 2018; 67:873–883.
18. Salem R, Gilbertsen M, Butt Z, et al. Increased quality of life among hepatocellular carcinoma patients treated with radioembolization, compared with chemoembolization. Clin Gastroenterol Hepatol 2013; 11: 1358–1365.e1.
19. Cremonesi M, Chiesa C, Strigari L, et al. Radioembolization of hepatic lesions from a radiobiology and dosimetric perspective. Front Oncol 2014; 4:210.
20. Strigari L, Sciuto R, Rea S, et al. Efficacy and toxicity related to treatment of hepatocellular carcinoma with 90Y-SIR spheres: radiobiologic considerations. J Nucl Med 2010; 51:1377–1385.
21. Elschot M, Vermolen BJ, Lam MG, de Keizer B, van den Bosch MA, de Jong HW. Quantitative comparison of PET and Bremsstrahlung SPECT for imaging the in vivo yttrium-90 microsphere distribution after liver radioembolization. PLoS One 2013; 8:e55742.
22. Lea WB, Tapp KN, Tann M, Hutchins GD, Fletcher JW, Johnson MS. Microsphere localization and dose quantification using positron emission tomography/CT following hepatic intraarterial radioembolization with yttrium-90 in patients with advanced hepatocellular carcinoma. J Vasc Interv Radiol 2014; 25:1595–1603.
23. Kao YH, Steinberg JD, Tay YS, et al. Post-radioembolization yttrium-90 PET/CT—part 2: dose-response and tumor predictive dosimetry for resin microspheres. EJNMMI Res 2013; 3:57.
24. Fowler KJ, Maughan NM, Laforest R, et al. PET/MRI of hepatic 90Y microsphere deposition determines individual tumor response. Cardiovasc Intervent Radiol 2016; 39:855–864.
25. Garin E, Lenoir L, Edeline J, et al. Boosted selective internal radiation therapy with 90Y-loaded glass microspheres (B-SIRT) for hepatocellular carcinoma patients: a new personalized promising concept. Eur J Nucl Med Mol Imaging 2013; 40:1057–1068.
26. Gil-Alzugaray B, Chopitea A, Iñarrairaegui M, et al. Prognostic factors and prevention of radioembolization-induced liver disease. Hepatology 2013; 57:1078–1087.
27. Emami B, Lyman J, Brown A, et al. Tolerance of normal tissue to therapeutic irradiation. Int J Radiat Oncol Biol Phys 1991; 21:109–122.
28. Kao YH, Tan EH, Ng CE, Goh SW. Clinical implications of the body surface area method versus partition model dosimetry for yttrium-90 radioembolization using resin microspheres: a technical review. Ann Nucl Med 2011; 25:455–461.
29. Chang TT, Bourgeois AC, Balius AM, Pasciak AS. Treatment modification of yttrium-90 radioembolization based on quantitative positron emission tomography/CT imaging. J Vasc Interv Radiol 2013; 24:333–337.
30. Garin E, Rolland Y, Laffont S, Edeline J. Clinical impact of 99mTc-MAA SPECT/CT-based dosimetry in the radioembolization of liver malignancies with 90Y-loaded microspheres. Eur J Nucl Med Mol Imaging 2016; 43: 559–575.

APPENDIX A. MATERIALS AND METHODS

Work-up Procedure

All patients underwent arteriography before treatment (work-up) to prepare and simulate the ^{90}Y injection that was performed 1–2 weeks later during the treatment procedure. The same interventional radiologist who performed the work-up performed the treatment procedure in 84% of cases (n = 38 of 45). The operators used the same catheter, microcatheters, and position of injection during both work-up and treatment procedures except in 3 cases (an additional embolization was needed in 1 case, and a better injection position was found during treatment in 2 cases). All procedures (whole-liver treatments) were lobar or segmental treatments except 2. When the tumor had invaded both lobes, treatment was performed with split injections during the same procedure (n = 5) or sequential lobar treatments (n = 4).

Whole-body planar scintigraphy and hepatic SPECT/CT (Infinia Hawkeye 4; GE Healthcare) were performed within 1 hour after the technetium-99m macroaggregated albumin injection to calculate lung shunt fraction, exclude any extrahepatic deposition, and estimate intrahepatic radiopharmaceutical distribution. The BSA method was used to calculate the required dose as follows: Activity (GBq) = $[(\text{BSA} - 0.2) + (V_{\text{tumor lobe}}/V_{\text{lobe}})] \times (V_{\text{lobe}}/V_{\text{liver}})$, with BSA ($m^2$) = $0.20247 \times \text{height}^{0.725}(m) \times \text{weight}^{0.425}(kg)$, and according to volumes of tumor in the treated lobe (V_{tumor}) and treated lobe (V_{lobe}) and total liver (V_{liver}). RE was contraindicated if the liver-to-lung shunt would result in > 25 Gy to the lungs (5). The activity calculation for repeated treatments was based on the same method with no dose reductions.

3D Dosimetry on PET/CT after ^{90}Y Injection

A PET/CT scan was performed within 24 hours after ^{90}Y injection (acquisitions of 2 bed positions, 40 minutes on a Biograph PET/CT) of all procedures. The delay between ^{90}Y RE and PET/CT was entered in the TPS for each treatment to consider ^{90}Y radiation decay. The PET reconstruction parameters used for RE dosimetry were 3D ordered-subset expectation maximization reconstruction algorithm with point spread function compensation, attenuation correction, Gaussian filter, 1 iteration/8 subsets, 128 × 128 matrix, and voxel size of 5.3 × 5.3 × 3.4 mm. Tumors < 1 cm were not considered for dose assessment because of partial volume effects in PET/CT imaging. 3D dosimetry was calculated in each case using a kernel convolution algorithm at a voxel level, based on the medical internal radiation dose formalism detailed in the Pamphlet No. 17 (7,8).

Statistical Analysis

Categorical variables were described by percentage. Continuous variables were expressed as mean ± SD or median (range). Group comparisons were made using Fisher exact test for categorical variables and a 2-sided *t* test or Kruskal-Wallis test as appropriate for continuous variables. Survival curves were estimated using the Kaplan-Meier method and compared using log-rank tests.

First, we compared mean $\text{AUDVH}_{\text{tumor}}$ in patients with tumor control versus progressive disease using the Mann-Whitney test. Then, univariate and multivariate logistic regression were performed to compute corresponding odds ratios (with 95% confidence intervals). Log linearity was checked using fractional polynomials. Second, the dose-response relationship was determined using a nonlinear regression model (9). Several theoretical models were evaluated, including log-logistic with 4 or 5 parameters, Gompertz with 3 or 4 parameters, and exponential with 2 or 3 parameters. A model using fractional polynomials was also evaluated. The models were compared using residual variance Akaike information criterion. The most parsimonious model was adopted for these criteria. Third, Pearson correlation coefficient (and 95%confidence interval) was calculated between $\text{AUDVH}_{\text{tumor - PVI}}$ and $\text{AUDVH}_{\text{PVI}}$. Agreement was estimated using the 95% limit-of-agreement method developed by Bland and Altman (10). We also determined Lin's concordance coefficient correlation (ρc) (11), which combines the measurements of precision and accuracy to determine whether the observed data deviate significantly from the line of perfect concordance (ie, the 45° line). Receiver operating characteristic analysis was performed to identify the optimal cutoff (defined by the Youden index) of AUDVH to predict tumor control. Finally, survival curves were estimated using the Kaplan-Meier method and compared using the log-rank test. All analyses were performed using Stata 14 and R software. $P < .05$ was considered to be significant.

RESULTS

Two procedures were excluded because 1 patient underwent liver transplantation 2 weeks after treatment making it impossible to perform response and toxicity evaluations, and 1 patient had 2 repeated injections in the same lobe. Another patient had a large HCC on the Cantlie line that was vascularized from both the right and the left hepatic arteries. This was treated by 2 separate injections over a 2-month interval. No significant overlap of the 2 injections was identified on ^{90}Y PET, and complete tumor targeting was obtained, so we analyzed both injections as a single treatment based on fusion of the 2 ^{90}Y PET/CT acquisitions. Tumor recurrence occurred in the nontreated liver of 2 patients 9 and 14 months after the first treatment, respectively. Each treatment was considered independently as if it had been for different patients. Consequently, 42 procedures were considered for dosimetric analysis, and 37 patients were considered for survival analysis. None of the patients received sorafenib or any targeted therapy or immunotherapy during the selective internal radiation therapy procedure.

Dose to Portal Vein Invasion

Portal vein invasion (PVI) was segmented from the main portal vein to the sectorial portal branches before segmental bifurcations. Thus, the 3 volumes (V_{liver}, V_{tumor}, and V_{PVI}) were imported into the TPS. $V_{tumor\ -\ PVI}$ represented the tumor volume without venous invasion and was obtained by subtracting V_{PVI} from V_{tumor}. DVHs of each anatomically defined volume (V_{tumor}, V_{PVI}, and their subtraction $V_{tumor\ -\ PVI}$) were obtained. AUDVHs ($AUDVH_{tumor}$, $AUDVH_{PVI}$, $AUDVH_{tumor\ -\ PVI}$), expressed in Gy, were calculated to measure the exposure of each tissue to ^{90}Y radiation. Dose delivered to PVI ($AUDVH_{PVI}$) and dose delivered to the tumor ($AUDVH_{tumor\ -\ PVI}$) were both highly correlated ($r = 0.82$; $P < .001$) and concordant ($\rho c = 0.802$; $P < .001$) (Fig E3). On Bland-Altman analysis, 93.75% (15 of 16) of points were within the limits of agreement.

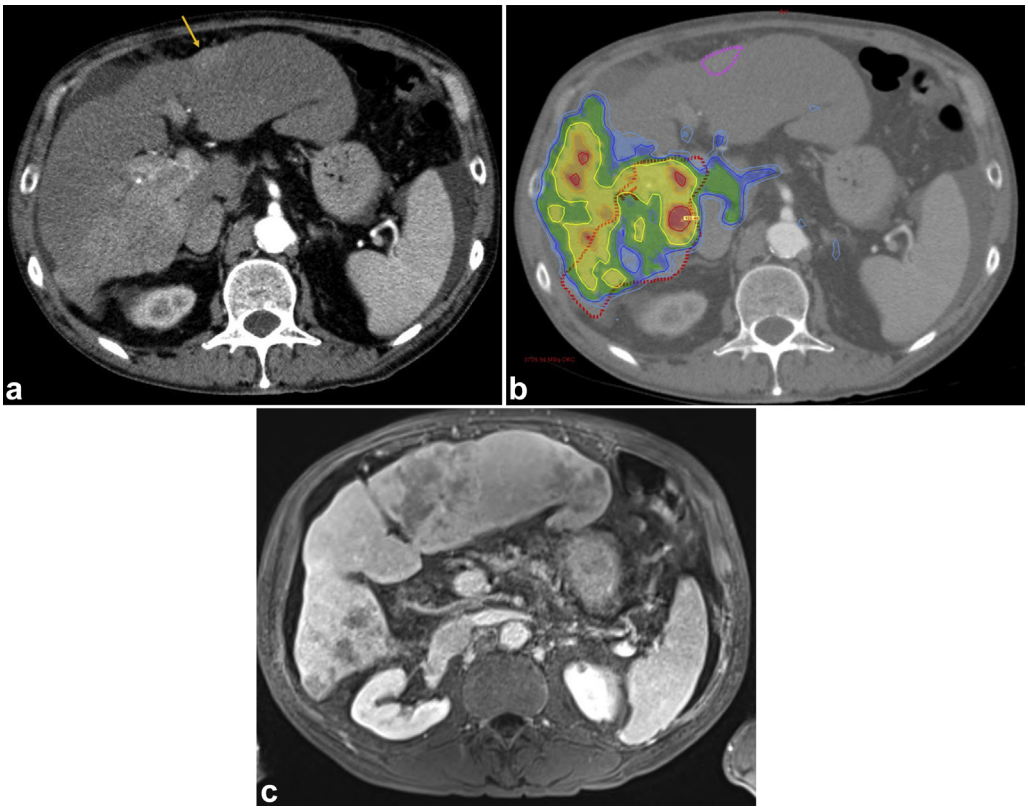

Figure E1. Example of incomplete targeting (limited contralateral disease). **(a)** Baseline CT scan with infiltrative HCC in the right lobe with right portal vein invasion and a small HCC nodule in the left lobe (arrow). **(b)** ^{90}Y PET/CT performed after RE in the right liver lobe shows good targeting of both infiltrative HCC and right portal vein invasion. **(c)** Magnetic resonance imaging performed 6 months after RE shows partial response in the right lobe but great progression of HCC in the left lobe.

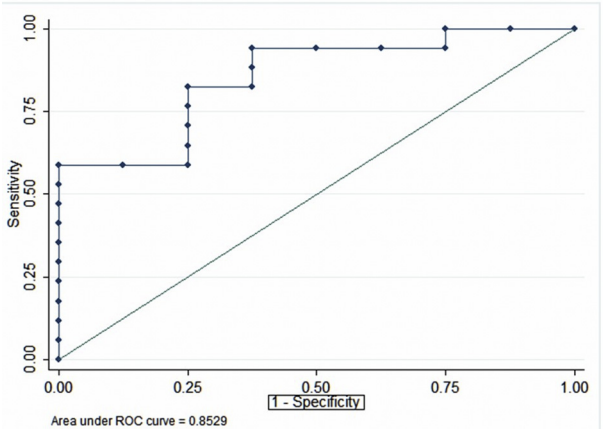

Figure E2. Receiver operating characteristic analysis for AUDVH to predict tumor control. ROC = receiver operating characteristic.

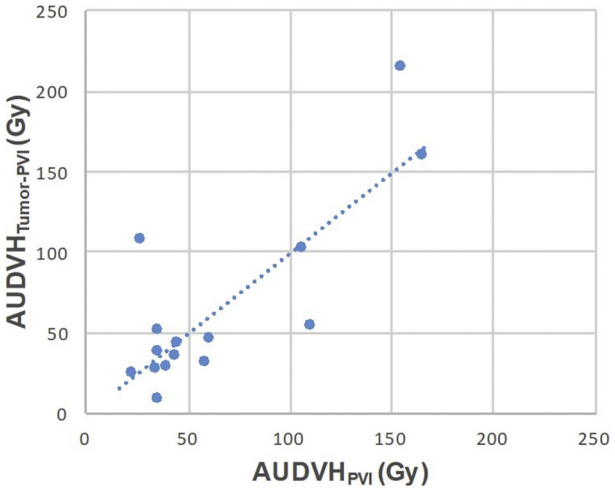

Figure E3. Correlation between the dose delivered to portal vein invasion ($AUDVH_{PVI}$) vs the tumor ($AUDVH_{tumor - PVI}$) ($r = 0.82$; $P < .001$).

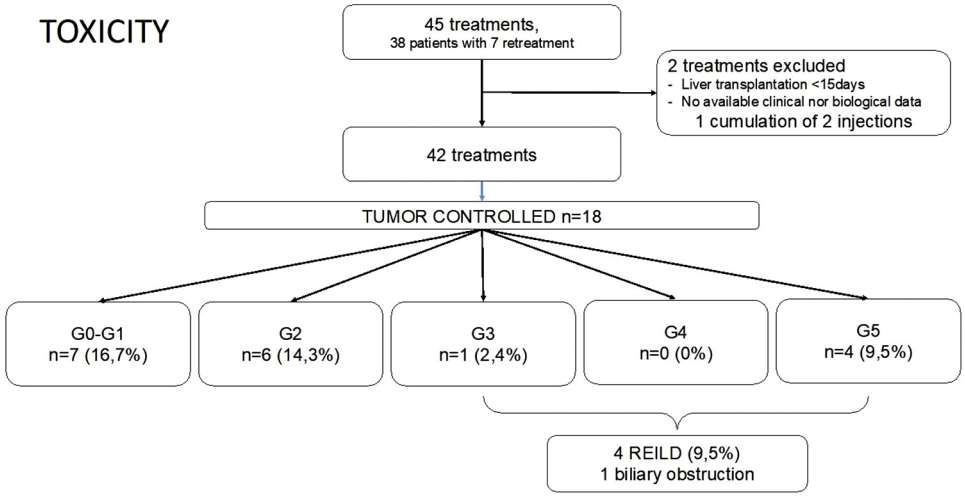

Figure E4. Flow chart showing Common Terminology Criteria for Adverse Events v4.0 grading of patients with tumor controlled and REILD. G = grade.